Combined Crossed Molecular Beams and Ab Initio Study of the Bimolecular Reaction of Ground State Atomic Silicon (Si; ^3P) with Germane (GeH_4; X^1A_1)

Vladislav S. Krasnoukhov,[a] Valeriy N. Azyazov,[a] Alexander M. Mebel,*[b] Srinivas Doddipatla,[c] Zhenghai Yang,[c] Shane Goettl,[c] and Ralf I. Kaiser*[c]

The chemical dynamics of the elementary reaction of ground state atomic silicon (Si; ^3P) with germane (GeH_4; X^1A_1) were unraveled in the gas phase under single collision condition at a collision energy of 11.8 ± 0.3 kJ mol^{-1} exploiting the crossed molecular beams technique contemplated with electronic structure calculations. The reaction follows indirect scattering dynamics and is initiated through an initial barrierless insertion of the silicon atom into one of the four chemically equivalent germanium-hydrogen bonds forming a triplet collision complex ($HSiGeH_3$; ^{3}**i1**). This intermediate underwent facile intersystem crossing (ISC) to the singlet surface ($HSiGeH_3$; ^{1}**i1**). The latter isomerized via at least three hydrogen atom migrations involving exotic, hydrogen bridged reaction intermediates eventually leading to the H_3SiGeH isomer **i5**. This intermediate could undergo unimolecular decomposition yielding the di-bridged butterfly-structured isomer ^{1}**p1** (Si(μ-H_2)Ge) plus molecular hydrogen through a tight exit transition state. Alternatively, up to two subsequent hydrogen shifts to **i6** and **i7**, followed by fragmentation of each of these intermediates, could also form ^{1}**p1** (Si(μ-H_2)Ge) along with molecular hydrogen. The overall non-adiabatic reaction dynamics provide evidence on the existence of exotic dinuclear hydrides of main group XIV elements, whose carbon analog structures do not exist.

1. Introduction

For more than a century, Langmuir's concept of isovalency has been exploited to establish concepts of chemical bonding and to interpret the molecular structures of isovalent molecules.[1] Notable attention has been given on elucidating the similarities and disparities of the chemistries of germanium and silicon with analogous carbon compounds.[2–5] Carbon, silicon, and germanium belong to main group 14 and hence are isovalent with four valence electrons each. According to Langmuir's concept, one can expect a planar D_{2h} symmetric structure as a global minimum on the Si_2H_4 and Ge_2H_4 potential energy surfaces (PESs) similar to the ethylene molecule (C_2H_4, (**1**)). However, the thermodynamically most stable geometries of the Si_2H_4 and Ge_2H_4 PES are quite distinct from the carbon analog structure (Scheme 1). On the Si_2H_4 PES, a non-planar, trans-bent C_{2h} symmetric structure (Si_2H_4, (**3**)) carrying sp^3 hybridized silicon atoms represents the energetically most favorable isomer.[6–10] Similarly, trans-bent Ge_2H_4 is thermodynamically the most stable isomer carrying sp^3 hybridized germanium atoms (Ge_2H_4; (**8**)).[11–14] The distinct chemical bonding of carbon versus silicon and germanium is further recognized by the comparison of the structures of acetylene (C_2H_2; (**13**)) with its higher row analogs (Scheme 2). The linear acetylene molecule (C_2H_2; (**13**)) is the most stable isomer on the C_2H_2 PES[15]; once one of the carbon atoms is replaced by silicon or germanium, silavinyli-

[a] V. S. Krasnoukhov, Prof. Dr. V. N. Azyazov
Samara National Research University,
Samara 443086
and
Lebedev Physical Institute,
Samara 443011, Russian Federation
[b] Prof. Dr. A. M. Mebel
Department of Chemistry and Biochemistry,
Florida International University,
Miami, FL 33199, USA
and
Samara National Research University,
Samara 443086
E-mail: mebela@fiu.edu
[c] Dr. S. Doddipatla, Dr. Z. Yang, S. Goettl, Prof. Dr. R. I. Kaiser
Department of Chemistry,
University of Hawai'i at Mānoa,
Honolulu, HI 96822, USA
E-mail: ralfk@hawaii.edu

Supporting information for this article is available on the WWW under https://doi.org/10.1002/cphc.202100235

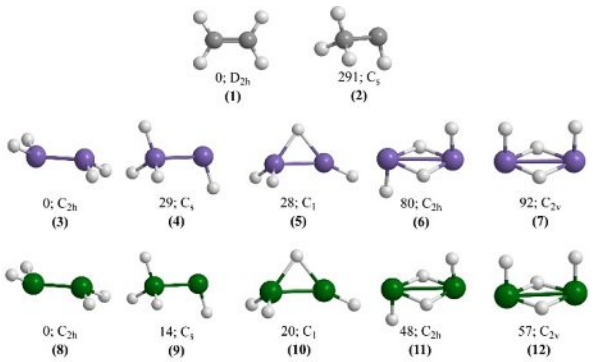

Scheme 1. Structures, point groups, and relative energies (kJ mol^{-1}) of homo- and heteroatomic dinuclear dihydrides of main group 14 elements. Atoms are color coded in gray (carbon), purple (silicon), green (germanium), and white (hydrogen).

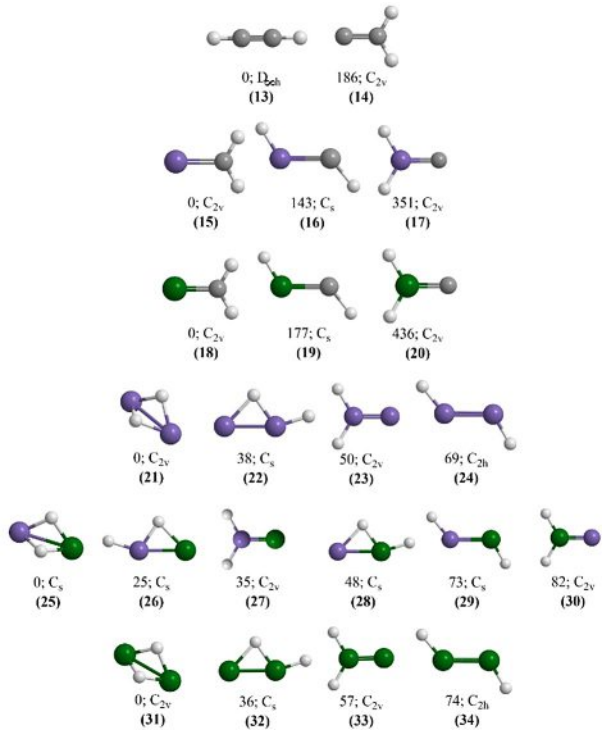

Scheme 2. Structures, point groups, and relative energies (kJ mol^{-1}) of homonuclear, dinuclear tetrahydrides of main group 14 elements. Atoms are color coded in gray (carbon), purple (silicon), green (germanium), and white (hydrogen).

dene (H_2CSi; (**15**))[16–18] and germavinylidene (H_2CGe; (**18**)) represent the global minima.[19] Isomers of homo- and heteronuclear hydrides carrying silicon and germanium, i.e. Si_2H_2, $SiGeH_2$, and Ge_2H_2, depict double-bridged butterfly structures - Si(μ-H_2)Si; (**21**), Si(μ-H_2)Ge; (**25**), Ge(μ-H_2)Ge; (**31**) - as the most stable isomers.[19–25] The linear species HSiSiH, HSiGeH, and HGeGeH represent transition states, but the trans-bent structures (HSiSiH; (**24**), HGeGeH; (**34**), HGeSiH; (**29**)) define local minima.

These 'simple' molecules with only four atoms show peculiar chemical bonding and molecular structures when replacing carbon by the isovalent silicon and/or germanium, whose carbon counterparts do not exist. The exotic non-classical hydrogen-bridged homo nuclear Si(μ-H_2)Si (**21**), HSi(μ-H)Si (**22**), Ge(μ-H_2)Ge (**31**), and HGe(μ-H)Ge (**32**) species have been studied spectroscopically.[26–28] Yet, experimental investigations on heteronuclear species and of $SiGeH_2$ isomers have been quite limited. These include the preparation of silagermenylidene ($GeSiH_2$; (**27**)) species, in which the hydrogen atom(s) is/are replaced by bulky groups such as 2,4,6-triisopropylphenyl;[29,30] likewise, a recent crossed molecular beam study of atomic germanium (Ge; ^{3}P) with silane (SiH_4; X^1A_1) formed the most stable, double-bridged (Ge(μ-H_2)Si; (**25**)) isomer[25] thus indicating the preferential stability of hydrogen-bridged isomers. Here, we are expanding the investigations on hydrogenated, heteronuclear molecules formed under single collision conditions in the gas phase through the exploration of the elementary reaction of ground state atomic silicon (Si; ^{3}P) with germane (GeH_4; X^1A_1). These investigations explore the non-adiabatic reaction dynamics involving intersystem crossing from the triplet to the singlet surface and identify critical isomerization steps via hydrogen migration and ultimately molecular hydrogen loss leading at least to the thermodynamically most stable double-bridged Si(μ-H_2)Ge isomer (**25**). Since the $Si + GeH_4$ reactants explored in the present work reside ~125 kJ mol^{-1} higher in energy than $Ge + SiH_4$ investigated in the previous work,[25] we show that the $Si + GeH_4 \rightarrow$ Si(μ-H_2)$Ge + H_2$ reaction is highly exothermic, and all transition states and intermediates reside below the reactants thus making the formation of the exotic double-bridged (Ge(μ-H_2)Si molecule feasible even at extremely low temperatures.

Methods

Experimental Methods

The bimolecular reaction between ground state atomic silicon (Si; ^{3}P) and germane (GeH_4; X^1A_1) was studied under single collision conditions using a crossed molecular beam machine.[31] A pulsed supersonic molecular beam of ground state atomic silicon (Si; ^{3}P) was generated in situ by laser ablation of a rotating silicon rod at 266 nm (30 Hz, 10 mJ per pulse) and subsequently seeding the ablated silicon atoms in neon gas (99.999%; Specialty Gases of America) released by a piezoelectric valve operated at 60 Hz, a pulse width of 80 μs, a peak amplitude of −400 V, and a backing pressure of 4 atm. The neon seeded beam of silicon atoms was collimated by a skimmer and velocity selected by four-slit chopper wheel rotating at 120 Hz resulting in well-defined peak velocities (v_p) of 932 ± 15 ms^{-1} and speed ratios (*S*) of 5.4 ± 0.5. Laser induced fluorescence (LIF) reveals that all silicon atoms are present in the ground electronic state (^{3}P).[24] The velocity selected silicon beam is perpendicularly crossed by a pulsed supersonic beam of neat germane (GeH_4; X^1A_1; Air Liquide; 99.999%) with a peak velocity (v_p) 529 ± 5 ms^{-1} and speed ratio (*S*) 9.0 ± 0.7 at a collision energy (E_C) 11.8 ± 0.3 kJ mol^{-1} and a center of mass (CM) angle Θ_{CM} of 58.4 ± 0.5°. Peak velocities and speed ratios for the reactants along with the collision energy and center-of-mass angle are given in Table 1.

The triply differentially pumped rotatable detector within the plane of the two reactant beams consists of a Brink-type ionizer,[32] a quadrupole mass spectrometer (QMS), and a Daly-type ion counter.[33] The neutral reaction products are ionized by electron impact (80 eV, 2 mA); the resultant ions are then mass filtered by a quadrupole mass spectrometer and eventually detected by a Daly-type ion counter. Angular resolved time-of-flight (TOF) spectra were recorded at distinct laboratory (LAB) angles and integrated to obtain the product laboratory angular distribution. A forward-convolution routine was used to transform laboratory data into center-of-mass frame.[34,35] This iterative method exploits a user-defined center-of-mass (CM) translational energy $P(E_T)$ and angular $T(\theta)$ flux distribution, which are varied until a suitable fit of the TOF

Table 1. Peak velocities (v_p) and speed ratios (*S*) of ground state atomic silicon (Si(^{3}P)) and germane (GeH_4; X^1A_1) along with the collision energy (E_C) and center-of-mass angle (Θ_{CM}).

Beam	v_p [m s^{-1}]	*S*	E_C [kJ mol^{-1}]	Θ_{CM} [deg]
Si(^{3}P)	932 ± 15	5.4 ± 0.5		
GeH_4 (X^1A_1)	529 ± 5	9.0 ± 0.7	11.8 ± 0.3	58.4 ± 0.5

spectra and angular distribution are achieved. The CM functions define a product flux contour map which reveals the differential reactive cross section $I(u, \theta) \sim P(u) \times T(\theta)$ as intensity with respect to the angle θ and the CM velocity u.

Computational Details

Geometries of the reactants, products, intermediates, and transition states partaking in the ground state atomic silicon reaction with germane were optimized with the doubly-hybrid density functional theory (DFT) B2PLYPD3 method[36] and Dunning's correlation-consistent cc-pVTZ basis set.[37] Vibrational frequencies and zero-point vibrational energy corrections (ZPE) were evaluated at the same B2PLYPD3/cc-pVTZ level of theory. All connections between local minima and transition states were verified by intrinsic reaction coordinate (IRC) calculations. Refined energies were obtained by coupled cluster[38–41] CCSD(T)/CBS calculations, where the energies at the complete basis set limit were extrapolated[42] from the energies computed with the cc-pVTZ and cc-pVQZ Dunning's correlation-consistent basis sets. It should be noted that B2PLYPD3 is a state-of-the-art doubly-hybrid functional which is capable to give optimized geometries and vibrational frequencies close to those computed at the gold standard CCSD(T) level. The expected accuracy of the CCSD(T)/CBS//B2PLYPD3/cc-pVTZ + ZPE(B2PLYPD3/cc-pVTZ) relative energies is better than 4 kJ mol^{-1}.[43] Also, where available, we compared the optimized B2PLYPD3 geometries with those reported in the previous work on the Ge + SiH_4 reaction using the CCSD/cc-pVTZ method and found a very close agreement, within 0.01 Å for bond lengths and 1–2° for bond angles. GAUSSIAN 09[44] and MOLPRO[45] programs were used to carry out the DFT and coupled clusters calculations, whereas the minimum on the seam of crossing (MSX) between the triplet and singlet electronic states was located utilizing the NST code,[46] which employs the MSX optimization strategy described by Bearpark et al.[47]

Rice-Ramsperger-Kassel-Marcus (RRKM) theory[48] was used for the calculations of energy-dependent rate constants of unimolecular reaction steps on the $SiGeH_4$ singlet surface starting from the initial singlet intermediate **i1**. The rate constants were computed depending on the available internal energy of each species within the harmonic approximation at a zero-pressure limit corresponding to crossed molecular beams conditions using B2PLYPD3/cc-pVTZ frequencies and employing our in-house code UNIMOL.[49] The RRKM rate constants were then used to compute product branching ratios by solving first-order kinetic equations within steady-state approximation.[50]

2. Results

2.1. Laboratory Frame

For the reaction of ground state atomic silicon (Si; ^{3}P) with germane (GeH_4; X^1A_1), reactive scattering signal was recorded from mass to charge (m/z) of 108 to 100 considering the natural isotope abundances of silicon ^{28}Si (92.2%), ^{29}Si (4.7%), and ^{30}Si (3.1%) as well as germanium ^{70}Ge (20.4%), ^{72}Ge (27.3%), ^{73}Ge (7.7%), ^{74}Ge (36.7%), and ^{76}Ge (7.8%). Signal at m/z = 104 was found to hold the best signal-to-noise ratio; ion counts at m/z = 107 and 108 are too weak to monitor; this is in line with the low natural abundance of silicon and germanium isotopes as incorporated in m/z = 107 ($^{29}Si^{76}GeH_2$) and 108 ($^{30}Si^{76}GeH_2$) (Figure S1, Table S1). The time-of-flight (TOF) spectra recorded at m/z = 106–100 are indistinguishable after scaling; this indicates that these species originate from a single reaction channel, i.e. Si (28 amu) + GeH_4 (78 amu) → $SiGeH_2$ (104 amu) + H_2 (2 amu). In this context, it is important to note that the atomic hydrogen elimination channel leading to $SiGeH_3$ isomers is endoergic by at least 62 kJ mol^{-1};[51] this channel is therefore closed considering the experimental collision energy of 11.8 ± 0.3 kJ mol^{-1}. The ion counts at m/z = 100-106 originate from the $SiGeH_2$ products with a different combination of silicon and germanium isotopes (Table S1); lower m/z = 103–100 are generated via dissociative electron impact ionization of the m/z = 104 ($^{28}Si^{74}GeH_2$) parent product(s) along with their isotopically substituted counterparts. The resulting TOF spectra at m/z = 104 (Figure 1) are then integrated and normalized with respect to the center-of-mass (CM) angle thus yielding the laboratory angular distribution; this distribution is – at least from 43° to 68° - forward-backward symmetric around the CM angle (Figure 2). These results indicate that the reaction of ground state atomic silicon with germane involves indirect scattering dynamics through $SiGeH_4$ reaction intermediate(s). The unimolecular decomposition of the intermediate(s) via molecular hydrogen loss forms product(s) with molecular formula $^{28}Si^{74}GeH_2$ (hereafter: $SiGeH_2$).

2.2. Center-of-Mass Frame

The time-of-flight spectra and the LAB angular distribution obtained at m/z = 104 for the reaction of ground state atomic silicon (Si; ^{3}P) with germane (GeH_4; X^1A_1) were fit with a single product channel with mass combination of 104 amu ($SiGeH_2$) and 2 amu (H_2). The CM translational energy $P(E_T)$ and angular $T(\theta)$ flux distributions obtained from the fitting are depicted in Figure 3. The hatched areas represent the error limits determined within the 1σ error range of the LAB angular distribution. The maximum translational energy $E_{max} = 192 \pm 13$ kJ mol^{-1} (Figure 3) characterizes the sum of the reaction energy and collision energy for those molecules born without internal excitation. Therefore, considering the collision energy 11.8 ± 0.3 kJ mol^{-1}, a reaction energy of −180 ± 13 kJ mol^{-1} to from the $SiGeH_2$ isomer(s) and molecular hydrogen is obtained. The distribution maximum of the CM translational energy distribution peaks away from the zero at 38 ± 3 kJ mol^{-1}; this finding proposes a tight exit transition state leading to $SiGeH_2$ plus molecular hydrogen from the $SiGeH_4$ intermediate(s).[52] The CM angular distribution shows non-zero intensity over the complete angular range from 0° to 180°; the forward-backward symmetry implies a lifetime of the decomposing complex longer than the rotational period. The maximum at 90° suggests geometrical constraints of the exit transition state(s) with molecular hydrogen eliminating perpendicularly to the plane of the decomposing complex almost parallel to the total angular momentum vector.[53] Therefore, it can be concluded that the reaction proceeds via indirect reactive scattering dynamics leading to $SiGeH_2$ isomer(s) plus molecular hydrogen via $SiGeH_4$ intermediate(s). These conclusions are also reflected in the CM flux contour map I(θ,u) (Figure 4) which describes the intensity of

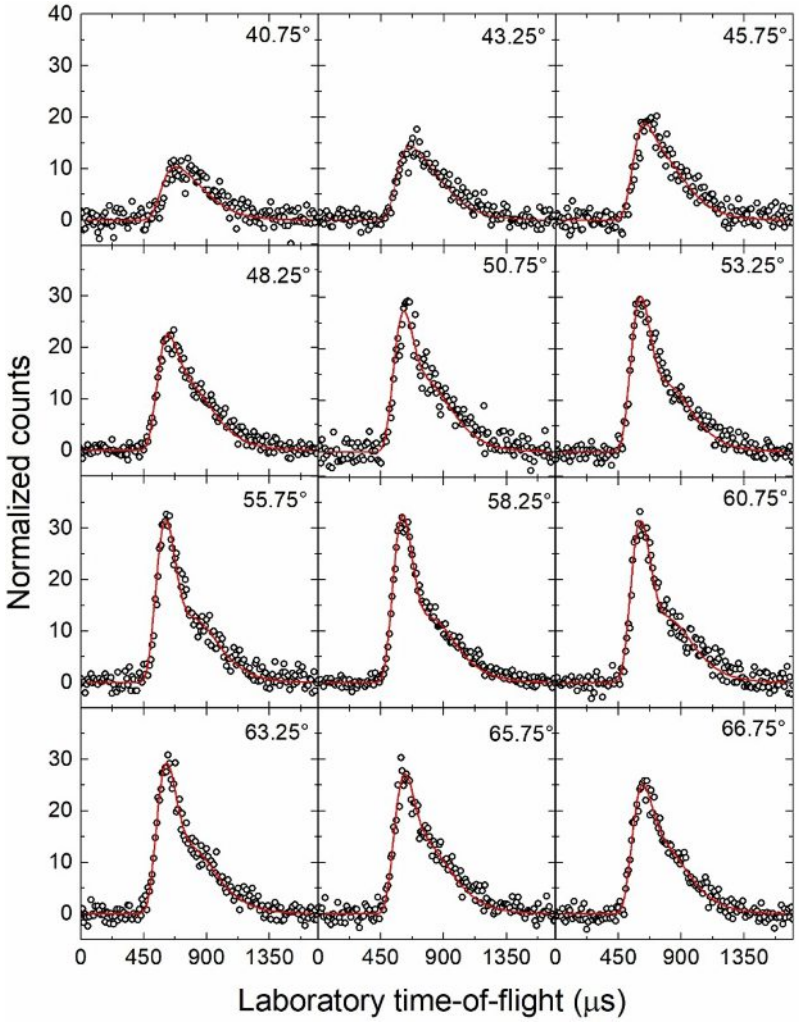

Figure 1. Time-of-flight (TOF) spectra recorded at $m/z = 104$ ($SiGeH_2^+$) for the reaction of ground state atomic silicon ($Si(^3P)$) with germane (GeH_4; X^1A_1). The circles are the experimental data and the red lines the best fits exploiting he center-of-mass functions (Figure 3).

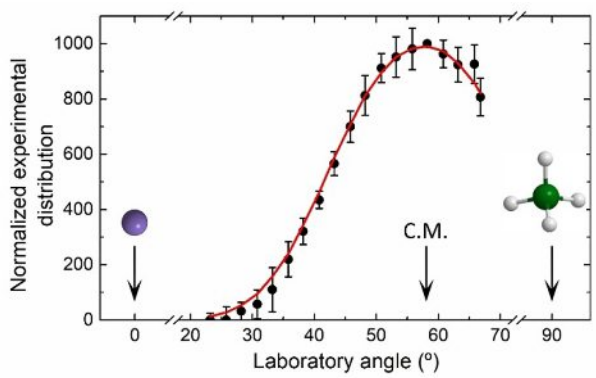

Figure 2. Laboratory angular distribution obtained at $m/z = 104$ ($SiGeH_2^+$) for the reaction of ground state atomic silicon ($Si(^3P)$) with germane (GeH_4; X^1A_1).). The circles are the experimental data and the red lines the best fits exploiting he center-of-mass functions (Figure 3).

the reactively scattered products as a function of the CM scattering angle (θ) and CM product velocity (u); mathematically, this is expressed as $I(\theta,u) \sim P(u)\ T(\theta)$ with the function $I(\theta,u)$ representing the reactive differential cross section. This provides a whole image of the measured reaction dynamics.

3. Discussion

To elucidate the reaction dynamics leading to the formation of $SiGeH_2$ isomer(s), we are combining the experimental data with results from electronic structure calculations. Based on the electronic structure calculations, six singlet $SiGeH_2$ isomers are energetically accessible (**^{1}p1**–**^{1}p6**; Figure 5). The experimentally obtained reaction energy of -180 ± 13 kJ mol^{-1} suggests the formation of at least the thermodynamically most stable double-bridged $SiGeH_2$ isomer **^{1}p1** ($Si(\mu\text{-}H_2)Ge$) revealing a computed reaction energy of -180 ± 4 kJ mol^{-1}. The existence of higher energy isomers **^{1}p2**-**^{1}p6** cannot be ruled out since their contributions might be masked in the low-energy part of the CM translational energy distribution. It is worth mentioning that the energies compiled in Figure 5 are presented for the

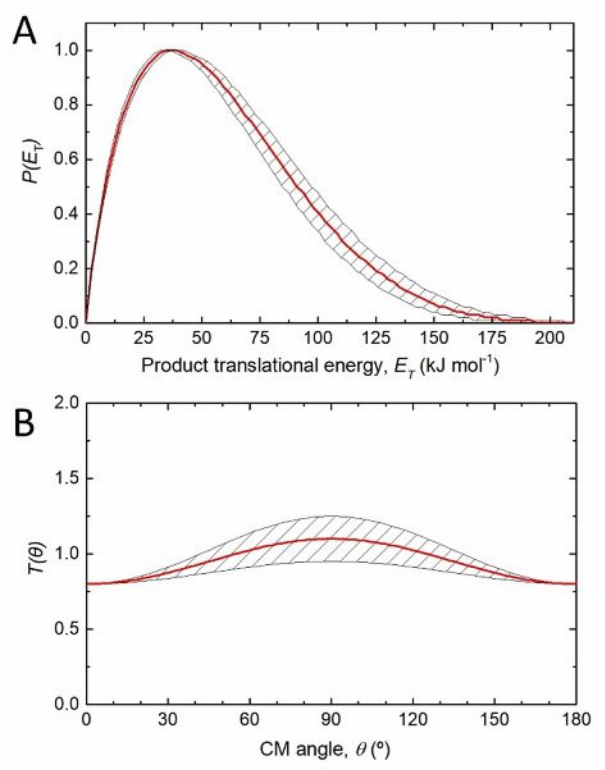

Figure 3. Center-of-mass translational energy (A) and angular (B) flux distributions for the formation of $SiGeH_2$ plus molecular hydrogen via the reaction of ground state atomic silicon ($Si(^3P)$) with germane (GeH_4; X^1A_1). The hatched areas define regions of acceptable fits.

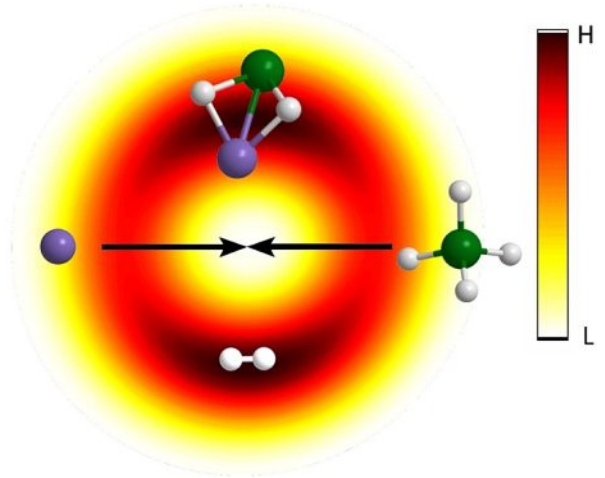

Figure 4. Top view of the flux contour map of the molecular hydrogen loss pathway in the reaction of ground state atomic silicon ($Si(^3P)$) with germane (GeH_4; X^1A_1) leading to the formation of $Si(\mu\text{-}H_2)Ge$. The color bar indicates the flux gradient from high (H) intensity to low (L) intensity. Color of atom: silicon (purple), germanium (green), and hydrogen (white).

ground electronic state of atomic silicon (Si; $^3P_0$). The j = 1 and 2 states are 0.9 and 2.7 kJ mol^{-1} higher in energy, respectively.[54] This would change the computed reaction energy to form ^{1}**p1** to -181 ± 4 and -183 ± 4 kJ mol^{-1}, which is still in excellent agreement with the experimental value of -180 ± 13 kJ mol^{-1}. It is important to note that the reactions between ground state silicon atoms (Si; ^3P) and germane (GeH_4; X^1A_1) commence on the triplet surface; however, both products ^{1}**p1** and molecular hydrogen have a singlet ground state. This finding indicates that intersystem crossing (ISC) from the triplet to the singlet manifold and hence non-adiabatic reaction dynamics drive the formation of ^{1}**p1** ($Si(\mu\text{-}H_2)Ge$) plus molecular hydrogen.

In detail, the electronic structure calculations predicted that the reaction of ground state atomic silicon (Si; ^3P) with germane (GeH_4; X^1A_1) starts on the triplet surface through barrierless insertion of atomic silicon into one of the germanium-hydrogen bonds yielding intermediate ^{3}**i1** stabilized by 134 kJ mol^{-1} relative to reactants. The calculations predict that intermediate ^{3}**i1** undergoes intersystem crossing (ISC) involving the minimum-on-the-seam-of-crossing (MSX) located only 0.1 kJ mol^{-1} below the ^{3}**i1** structure to intermediate **i1** on the singlet surface; this intermediate resides 236 kJ mol^{-1} below the energy of the separated reactants. The geometry of MSX is rather similar to that of ^{3}**i1**, with the only notable difference being the increase of the HSiGe bond angle from 120.7° in ^{3}**i1** to 127.5° in MSX. On the singlet surface, nine intermediates are identified. Intermediate **i1** opens three isomerization channels: (i) hydrogen migration from germanium to the silicon atom via a transition state located at 25 kJ mol^{-1} above intermediate **i1** forms the $SiGeH_4$ isomer **i2** with both silicon and germanium being sp^3 hybridized, (ii) hydrogen atom migration from the germanium atom forms a bridging hydrogen bond between silicon-germanium **i9** via a transition state located at 9 kJ mol^{-1} above intermediate **i1**, and (iii) two hydrogen atoms attached to the germanium form a double-bridged intermediate **i6** through a high energy transition state located 126 kJ mol^{-1} above intermediate **i1**. These intermediates can isomerize further. Intermediate **i2** could undergo two isomerization processes through hydrogen migration eventually leading to two bridged isomers **i4** and **i9**. Additional hydrogen migrations can lead to **i5** from **i4**, **i6** from **i5**, **i8** from **i6**, **i9** from **i6** or **i7**, and **i3** from **i9**. Intermediates **i6** and **i7** are connected via cis-trans isomerization.

With respect to the identification of at least the thermodynamically most stable product ^{1}**p1** ($Si(\mu\text{-}H_2)Ge$), our calculations reveal five possible exit channels from the decomposing intermediates. First, intermediate **i5** can undergo molecular hydrogen loss while simultaneously forming two silicon-carbon bridges; this significant electron reorganization is connected with a tight exit transition state located 76 kJ mol^{-1} above the separated products. Intermediate **i4** also undergoes extensive reorganization of the molecular structure upon molecular hydrogen loss and formation of a second germanium-silicon bridge resulting in a tight exit transition state 128 kJ mol^{-1} above the separated products. In decomposing intermediates **i6** and **i7**, both hydrogen bridged silicon-germanium moieties already exist, resulting in somewhat lower, but still tight, exit transition states placed 80 and 84 kJ mol^{-1} above the separated products, respectively. Finally, intermediate **i9** may fragment under simultaneous formation of a second hydrogen bridged germanium-silicon moiety and elimination of molecular hydro-

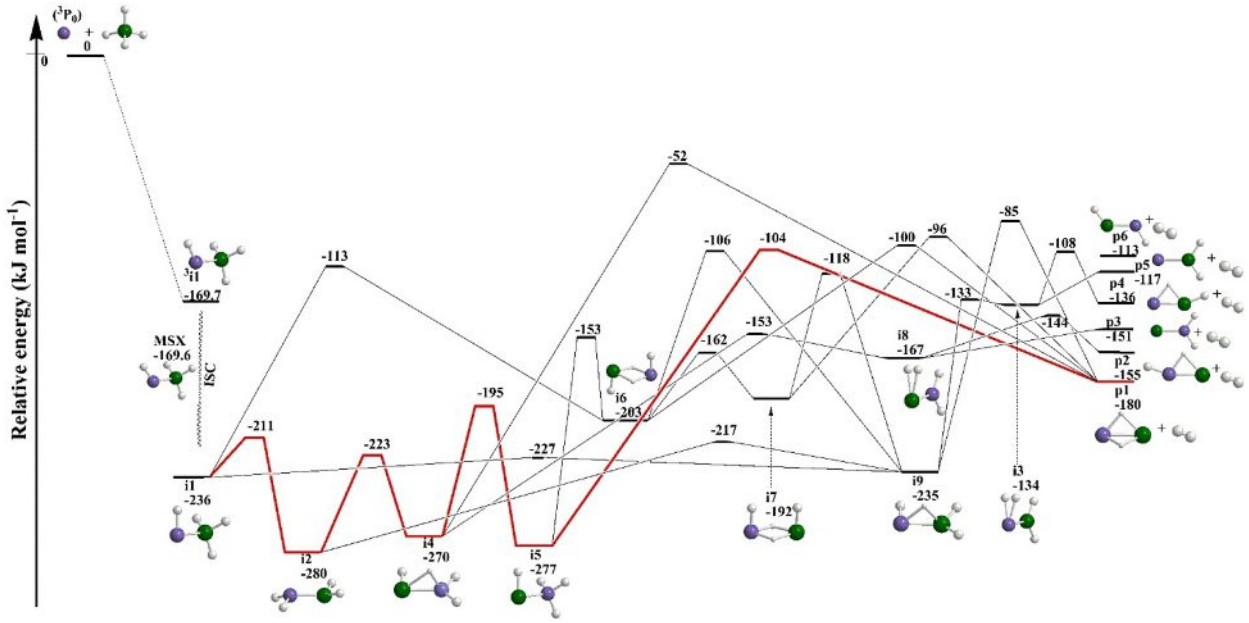

Figure 5. Potential energy surface for the reaction of ground-state atomic silicon (Si; ^{3}P) and germane (GeH_4; X^1A_1). Relative energies are given in units of kJ mol^{-1}. Atoms are color coded in purple (silicon), green (germanium), and white (hydrogen). Red pathways represent the dominating route to ^{1}**p1** based on our study.

gen, also through at tight exit transition state located 95 kJ mol^{-1} above the separated products. Overall, all five exit transition states leading to ^{1}**p1** (Si(μ-H_2)Ge) are tight. We can now compare the geometries of these exit transition states with the experimental finding that the dominating channel for the molecular hydrogen loss must involve a hydrogen emission nearly parallel to the total angular momentum vector almost perpendicularly to the plane of the decomposing intermediate. A detailed inspection of the geometries of these five exit transition states reveals that each of these transition states fulfills this condition with molecular hydrogen losses from **i4**, **i5**, and **i9** depicting angles close to 80° (Figure 6).

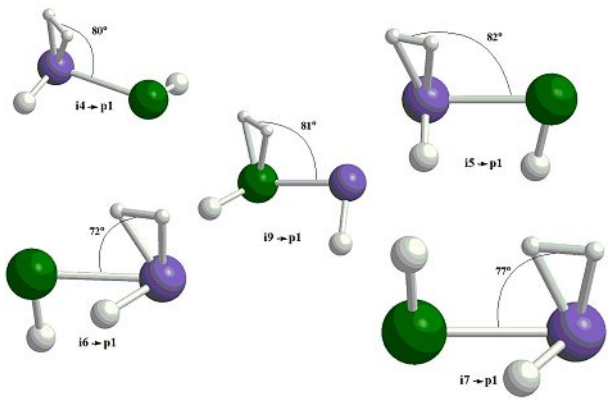

Figure 6. Geometries of the exit transition states leading to the thermodynamically most stable isomer ^{1}**p1** (Si(μ-H_2)Ge). Atoms are color coded in purple (silicon), green (germanium), and white (hydrogen).

Based on these findings, we may propose the following reaction dynamics leading to the formation of ^{1}**p1** (Si(μ-H_2)Ge) along with molecular hydrogen. The reaction is initiated by the barrierless insertion of ground state atomic silicon into one of the chemically equivalent germanium – hydrogen bonds of germane on the triplet surface leading to ^{3}**i1**. This intermediate undergoes intersystem crossing to the singlet surface forming **i1**. The intersystem crossing is feasible here for a number of reasons: First, the MSX geometric structure is rather similar to the structure of the ^{3}**i1** local minimum, the MSX energy is only 0.1 kJ mol^{-1} higher than that of ^{3}**i1** and thus, the crossing would occur in the close vicinity of the triplet isomer initially formed in the Si + GeH_4 reaction. Second, other fates of ^{3}**i1** are not competitive; the atomic hydrogen elimination channel from ^{3}**i1** leading to $SiGeH_3$ isomers is endoergic by at least 62 kJ mol^{-1}[51] is closed at the experimental collision energy of 11.8 kJ mol^{-1}, whereas the H_2 elimination from ^{3}**i1** on the triplet surface features high barriers of at least 139 kJ mol^{-1}. Moreover, the experimentally detected Si(μ-H_2)Ge (^{1}A′) + H_2 product can be formed only on the singlet PES, which corroborates the feasibility of the triplet-singlet intersystem crossing. Successive isomerization steps involving hydrogen migration to **i2**, a second hydrogen migration forming a hydrogen bridged intermediate **i4**, followed by a third hydrogen shift to **i5** have relatively low-lying transition states (≤ 75 kJ mol^{-1}) and hence can proceed easily. Intermediate **i5** can undergo unimolecular decomposition yielding ^{1}**p1** (Si(μ-H_2)Ge) plus molecular hydrogen through a tight exit transition state. Alternatively, isomerization of **i5** leads to **i6**, which either isomerizes to **i7** or emits molecular hydrogen forming ^{1}**p1** (Si(μ-H_2)Ge). **i7** may also eject molecular hydrogen through a tight exit transition state

forming the product ^{1}**p1** (Si(μ-H_2)Ge); complexes **i4** and **i9** also connect to ^{1}**p1** (Si(μ-H_2)Ge), but the energies of the exit transition states are less likely to compete with the aforementioned pathways. Statistical (RRKM) calculations verify these conclusions and reveal that ^{1}**p1** (Si(μ-H_2)Ge) is predominantly formed via decomposition of **i5** (82%), whereas decompositions of **i9** (7%) and **i6** and **i7** (~5 % each) give smaller contributions. Consequently, the identification of at least the thermodynamically most stable, dibridged isomer Si(μ-H_2)Ge involves non-adiabatic reaction dynamics and intersystem crossing from the triplet to the singlet surface, an initial barrierless insertion of ground state atomic silicon, at least three, possibly up to five consecutive hydrogen atom migrations via hydrogen bridged intermediates, and tight exit transition states with an inherent significant electron reorganization upon formation of the reaction products under single collision conditions.

4. Conclusions

The reaction of ground state atomic silicon (Si; ^{3}P) with germane (GeH_4; X^1A_1) was explored in the gas phase under single collision condition at a collision energy of 11.8 ± 0.3 kJ mol^{-1} exploiting the crossed molecular beams technique combined with electronic structure calculations. The reaction is dictated by indirect scattering dynamics through an initial insertion of the silicon atom into one of the four chemically equivalent germanium-hydrogen bonds leading to a triplet reaction intermediate ^{3}**i1**. This intermediate underwent facile intersystem crossing (ISC) in close vicinity of ^{3}**i1** to the singlet surface yielding intermediate **i1**. The latter underwent at least three consecutive hydrogen atom migrations involving exotic, hydrogen bridged reaction intermediates eventually leading to **i5**. The latter could undergo unimolecular decomposition yielding ^{1}**p1** (Si(μ-H_2)Ge) plus molecular hydrogen through a tight exit transition state. Alternatively, up to two subsequent hydrogen shifts to **i6** and **i7**, followed by fragmentation of each of these intermediates, could also form ^{1}**p1** (Si(μ-H_2)Ge) along with molecular hydrogen. Note that the formation of higher energy isomers (^{1}**p2**-^{1}**p6**) cannot be ruled out. These results underline the non-adiabatic reaction dynamics in the unimolecular decomposition of dinuclear hydrides of main group XIV elements leading to exotic, bridged molecular structures, which do not exist in their isovalent carbon counterparts.

Acknowledgments

The experimental studies were supported by the US National Science Foundation (NSF) for support under award CHE-1853541. Ab initio calculations at Samara University were supported by the Ministry of Science and Higher Education of the Russian Federation by the grant No. 14.Y26.31.0020.

Conflict of Interest

The authors declare no conflict of interest.

Keywords: isovalency · dinuclear hydrides · chemical dynamics · non-adiabatic · density functional calculations

[1] I. Langmuir, *J. Am. Chem. Soc.* **1919**, *41*, 568–934.
[2] H. Lischka, H.-J. Köhler, *J. Am. Chem. Soc.* **1983**, *105*, 6646–6649.
[3] J. S. Binkley, *J. Am. Chem. Soc.* **1984**, *106*, 603–609.
[4] Z. Palágyi, H. F. Schaefer, III, E. Kapuy, *J. Am. Chem. Soc.* **1993**, *115*, 6901–6903.
[5] Y. Wang, Y. Xie, P. Wei, R. B. King, H. F. Schaefer, III, P. v. R. Schleyer, G. H. Robinson, *Science* **2008**, *321*, 1069–1071.
[6] G. Olbrich, *Chem. Phys. Lett.* **1986**, *130*, 115–119.
[7] R. A. Poirier, J. D. Goddard, *Chem. Phys. Lett.* **1981**, *80*, 37–41.
[8] G. Dolgonos, *Chem. Phys. Lett.* **2008**, *466*, 11–15.
[9] L. Sari, M. C. McCarthy, H. F. Schaefer, III, P. Thaddeus, *J. Am. Chem. Soc.* **2003**, *125*, 11409–11417.
[10] B. T. Luke, J. A. Pople, M.-B. Krogh-Jespersen, Y. Apeloig, M. Kami, J. Chandrasekhar, P. v. R. Schleyer, *J. Am. Chem. Soc.* **1986**, *108*, 270–284.
[11] W. Carrier, W. Zheng, Y. Osamura, R. I. Kaiser, *Chem. Phys.* **2006**, *330*, 275–286.
[12] G. Trinquier, *J. Am. Chem. Soc.* **1990**, *112*, 2130–2137.
[13] G. Trinquier, J.-P. Malrieu, P. Riviere, *J. Am. Chem. Soc.* **1982**, *104*, 4529–4533.
[14] S. Nagase, T. Kudo, *J. Mol. Struct.* **1983**, *103*, 35–44.
[15] J. A. DeVine, M. L. Weichman, X. Zhou, J. Ma, B. Jiang, H. Guo, D. M. Neumark, *J. Am. Chem. Soc.* **2016**, *138*, 16417–16425.
[16] T. Lu, Q. Hao, J. J. Wilke, Y. Yamaguchi, D.-C. Fang, H. F. Schaefer, III, *J. Mol. Struct.* **2012**, *1009*, 103–110.
[17] M. R. Hoffmann, Y. Yoshioka, H. F. Schaefer, III, *J. Am. Chem. Soc.* **1983**, *105*, 1084–1088.
[18] A. C. Hopkinson, M. H. Lien, I. G. Csizmadia, *Chem. Phys. Lett.* **1983**, *95*, 232–234.
[19] A. J. Boone, D. H. Magers, J. Leszczynski, *Int. J. Quantum Chem.* **1998**, *70*, 925–932.
[20] M. Lein, A. Krapp, G. Frenking, *J. Am. Chem. Soc.* **2005**, *127*, 6290–6299.
[21] J. M. Galbraith, H. F. Schaefer, III, *J. Mol. Struct.* **1998**, *424*, 7–20.
[22] K. T. Petrov, T. Veszprémi, *Int. J. Quantum Chem.* **2009**, *109*, 2526–2541.
[23] P. O'Leary, J. R. Thomas, H. F. Schaefer, III, B. J. Duke, B. O'Leary, *Int. J. Quantum Chem. Quantum Chem. Symp.* **1995**, *29*, 593–604.
[24] T. Yang, B. B. Dangi, R. I. Kaiser, K.-H. Chao, B.-J. Sun, A. H. H. Chang, T. L. Nguyen, J. F. Stanton, *Angew. Chem. Int. Ed.* **2017**, *56*, 1264–1268; *Angew. Chem.* **2017**, *129*, 1284–1288.
[25] A. M. Thomas, B. B. Dangi, T. Yang, G. R. Tarczay, R. I. Kaiser, B.-J. Sun, S.-Y. Chen, A. H. H. Chang, T. L. Nguyen, J. F. Stanton, A. M. Mebel, *J. Phys. Chem. Lett.* **2019**, *10*, 1264–1271.
[26] M. Bogey, H. Bolvin, C. Demuynck, J. L. Destombes, *Phys. Rev. Lett.* **1991**, *66*, 413–416.
[27] M. Cordonnier, M. Bogey, C. Demuynck, J.-L. Destombes, *J. Chem. Phys.* **1992**, *97*, 7984–7989.
[28] X. Wang, L. Andrews, G. P. Kushto, *J. Phys. Chem. A* **2002**, *106*, 5809–5816.
[29] A. Jana, V. Huch, D. Scheschkewitz, *Angew. Chem. Int. Ed.* **2013**, *52*, 12179–12182; *Angew. Chem.* **2013**, *125*, 12401–12404.
[30] A. Jana, M. Majumdar, V. Huch, M. Zimmer, D. Scheschkewitz, *Dalton Trans.* **2014**, *43*, 5175–5181.
[31] R. I. Kaiser, P. Maksyutenko, C. Ennis, F. Zhang, X. Gu, S. P. Krishtal, A. M. Mebel, O. Kostko, M. Ahmed, *Faraday Discuss.* **2010**, *147*, 429–478.
[32] G. O. Brink, *Rev. Sci. Instrum.* **1966**, *37*, 857–860.
[33] N. R. Daly, *Rev. Sci. Instrum.* **1960**, *31*, 264–267.
[34] W. P. Storch, Ph. D. Dissertation Thesis, University of California, Berkeley, CA, **1986**.
[35] M. F. Vernon, Ph. D. Dissertation Thesis, University of California Berkeley, CA, **1983**.
[36] a) S. Grimme, *J. Chem. Phys.* **2006**, *124*, 034108; b) L. Goerigk, S. Grimme, *J. Chem. Theory Comput.* **2011**, *7*, 291–309; c) S. Grimme, S. Ehrlich, L. Goerigk, *J. Comput. Chem.* **2011**, 32, 1456–1465.
[37] T. H. Dunning, Jr., *J. Chem. Phys.* **1989**, *90*, 1007–1023.
[38] G. D. Purvis III, R. J. Bartlett, *J. Chem. Phys.* **1982**, *76*, 1910–1918.

[39] C. Hampel, K. A. Peterson, H.-J. Werner, *Chem. Phys. Lett.* **1992**, *190*, 1–12.
[40] P. J. Knowles, C. Hampel, H.-J. Werner, *J. Chem. Phys.* **1993**, *99*, 5219–5227.
[41] M. J. Deegan, P. J. Knowles, *Chem. Phys. Lett.* **1994**, *227*, 321–326.
[42] J. M. L. Martin, O. Uzan, *Chem. Phys. Lett.* **1998**, *282*, 16–24.
[43] J. Zhang, E. F. Valeev, *J. Chem. Theory Comput.* **2012**, *8*, 3175–3186.
[44] M. Frisch, G. Trucks, H. Schlegel, G. Scuseria, M. Robb, J. Cheeseman, G. Scalmani, V. Barone, B. Mennucci, G. A. Petersson, et al., Gaussian 09, Revision D. 01, Gaussian, Inc.: Wallingford CT, **2009**.
[45] H.-J. Werner, P. Knowles, R. Lindh, F. Manby, M. Schütz, P. Celani, T. Korona, A. Mitrushenkov, G. Rauhut, *MOLPRO, version 2010.1, a package of ab initio programs*, University of Cardiff, Cardiff, UK, **2010**.
[46] A. W. Jasper, *NST, A Spin-Forbidden Nonadiabatic Flux Code*. Available at: https://tcg.cse.anl.gov/papr/codes/nst.html.
[47] M. J. Bearpark, M. A. Robb, H. B. Schlegel, *Chem. Phys. Lett.* **1994**, *223*, 269–274.
[48] a) P. J. Robinson, K. A. Holbrook, *Unimolecular reactions*, Wiley, New York, **1972**; b) H. Eyring, S. H. Lin, S. M. Lin, *Basic chemical kinetics*, John Wiley & Sons, New York, **1980**; c) J. I. Steinfeld, J. S. Francisco, W. L. Hase, Chemical kinetics and dynamics, Vol. 3, Prentice Hall, Englewood Cliffs, **1982**.
[49] C. He, L. Zhao, A. M. Thomas, A. N. Morozov, A. M. Mebel, R. I. Kaiser, *J. Phys. Chem. A* **2019**, *123*, 5446–5462.
[50] V. V. Kislov, T. L. Nguyen, A. M. Mebel, S. H. Lin, S. C. Smith, *J. Chem. Phys.* **2004**, *120*, 7008–7017.
[51] Z. Yang, S. Doddipatla, R. I. Kaiser, V. S. Krasnoukhov, V. N. Azyazov, A. M. Mebel, *ChemPhysChem* **2020**, *21*, 1–9.
[52] R. D. Levine, *Molecular Reaction Dynamics*. Cambridge University Press: U.K., **2005**.
[53] W. B. Miller, S. A. Safron, D. R. Herschbach, *Discuss. Faraday Soc.* **1967**, *44*, 108–122.
[54] W. C. Martin, R. Zalubas, *J. Phys. Chem. Ref. Data* **1983**, *12*, 323–380.

Manuscript received: March 29, 2021
Revised manuscript received: April 30, 2021
Accepted manuscript online: May 18, 2021
Version of record online: June 10, 2021